Biochemistry

 Volume 38, Number 41 October 12, 1999

Articles

Role of Metal Ions in the T- To R-Allosteric Transition in the Insulin Hexamer†

Webe Kadima*

Department of Chemistry, State University of New York at Oswego, Oswego, New York 13126

Received February 9, 1999; Revised Manuscript Received April 7, 1999

ABSTRACT: The role of metal ions in the T- to R-allosteric transition is ascertained from the investigation of the T- to R-allosteric transition of transition metal ions substituted−insulin hexamers, as well as from the kinetics of their dissociation. These studies establish that ligand field stabilization energy (LFSE), coordination geometry preference, and the Lewis acidity of the metal ion in the zinc sites modulate the T- to R-state transition. ^{1}H NMR, ^{113}Cd NMR, and UV−vis measurements demonstrate that, under suitable conditions, $Fe^{2+/3+}$, Ni^{2+}, and Cd^{2+} bind insulin to form stable hexamers, which are allosteric species. ^{1}H NMR R-state signatures are elicited by addition of phenol alone in the case of Ni(II)- and Cd(II)-substituted insulin hexamers. The Fe(II)-substituted insulin hexamer is converted to the ferric analogue upon addition of phenol. For the Fe(III)-substituted insulin hexamer, appearance of ^{1}H NMR R-state signatures requires, additionally to phenol, ligands containing a nitrogen that can donate a lone pair of electrons. This is consistent with stabilization of the R-state by heterotropic interactions between the phenol-binding pocket and ligand binding to Fe(III) in the zinc site. UV−vis measurements indicate that the ^{1}H NMR detected changes in the conformation of the Fe(III)−insulin hexamer are accompanied by a change in the electronic structure of the iron site. Kinetic measurements of the dissociation of the hexamers provide evidence for the modulation of the stability of the hexamer by ligand field stabilization effects. These kinetic studies also demonstrate that the T- to R-state transition in the insulin hexamer is governed by coordination geometry preference of the metal ion in the zinc site and the compatibility between Lewis acidity of the metal ion in the zinc site and the Lewis basicity of the exogenous ligands. Evidence for the alteration of the calcium site has been obtained from ^{113}Cd NMR measurements. This finding adds to the number of known conformational changes that occur during the T- to R-transition and is an important consideration in the formulation of allosteric mechanisms of the insulin hexamer.

The action of insulin in vivo, in the control of glucose metabolism, is initiated by the binding of monomeric insulin to the receptor. However, insulin is stored in the pancreas within granules where six molecules of insulin are complexed by zinc(II) ions. The zinc−insulin complex crystallized in vitro is known as the 2-zinc−insulin hexamer (*1*). Characterization of parameters and events that affect the dissociation of the hexamer and conformational changes of insulin is very important, because both the dissociation and conformational equilibrium are involved in the regulation of the function of insulin and the nature of insulin preparations.

The 2-zinc−insulin hexamer is an assembly of three equivalent dimers related by a 3-fold axis of symmetry (*1*). The hexamer is of torus shape with a height of 35 Å and a diameter of 50 Å as illustrated in Figure 1. Each slice in the cylindrical hexamer in Figure 1 represents a monomer. In

†This work was supported by Research Corporation Cotrell Science Award C-3762.

* To whom correspondence should be addressed. Phone: (315) 341-2746. Fax: (315) 341-5424. E-mail: kadima@oswego.edu.

10.1021/bi9903188 CCC: $18.00
Published on Web 09/17/1999

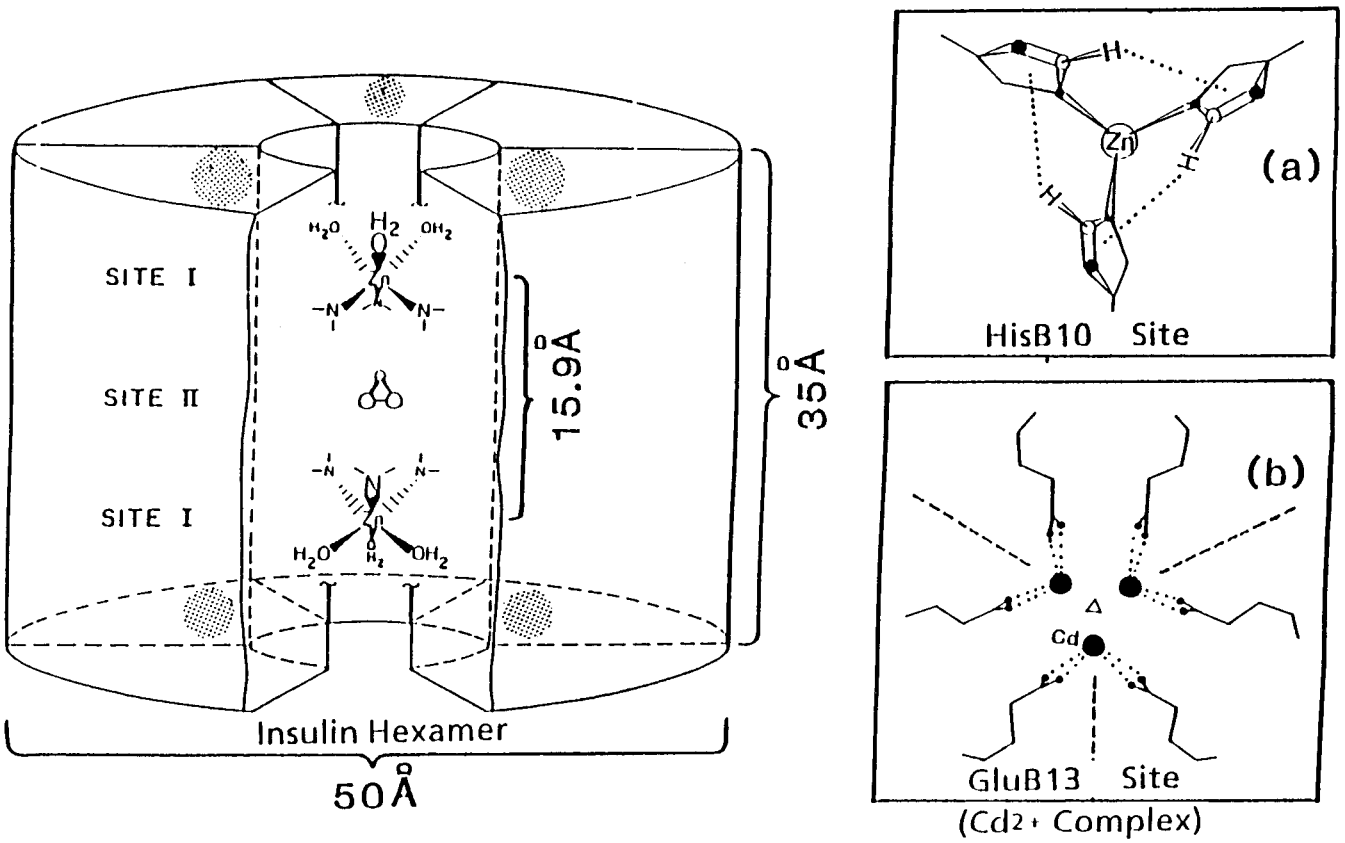

FIGURE 1: The cylindrical insulin hexamer (left) showing two types of metal-binding sites (I and II); the zinc-binding site is comprised of three histidines B10 residues (a) and the putative calcium-binding site, showing one-third occupation by Cd(II), is comprised of glutamate B13 residues (b). Redrawn with permission from ref *18*.

crystalline state, the two monomers in the dimer are related by a pseudo 2-fold axis of symmetry and are referred to as monomer 1 and monomer 2 to indicate that they are not equivalent (*1*). The two equivalent zinc binding sites (site I in the hexamer in Figure 1) are located along the 3-fold axis of symmetry and coordinated by three nitrogens from the imidazolyl side chains of three equivalent histidine B10 residues (Figure 1a). Water molecules or other exogenous ligands occupy the remaining coordination positions on zinc. The hexamer contains also a putative calcium-binding site located in the middle of the hexamer (site II in Figure 1), formed by the carboxylate groups of glutamate B13 residues. ^{113}Cd NMR[1] studies have demonstrated that the latter site can be occupied by Cd(II) (*2*). Although this site consists of six carboxylates capable of binding three Ca(II) (filled dots in Figure 1b), only one Cd(II) (triangle in Figure 1b) occupies this site as illustrated by the one-third occupancy (*2*).

The 2-zinc−insulin hexamer has been characterized as an allosteric protein exhibiting two extreme global protein conformations and metal ion binding geometries (*1*, *3*). In the hexamer, insulin subunits can fold into two distinct global conformations, known as T- and R-state conformations according to allosteric nomenclature. Figure 2 illustrates the two types of conformations and the coordination geometry of the zinc-binding site that is accommodated by each conformation. The folding shown in inset A is the T-conformation, in which the B chain from residue B1 to B8 assumes an extended conformation. The hexamer with the six monomeric units in the T-fold is referred to as the T_6, or more precisely as $T_3T_3'^2$ to signify pseudosymmetry within the dimer as observed in crystalline state (*1*). In the T_6 hexamer, the two zinc sites assume an octahedral coordination geometry (Figure 2A, panel b). When the insulin hexamer is crystallized in the presence of phenol and other phenol-like molecules, X-ray crystallographic studies show that the extended chain formed by residues B1 to B8 is transformed into a helix, thus rendering the B chain α-helical from residue B1 to B19 (*3*). The phenol-induced conformation, known as the R-state/conformation, is depicted in Figure 2B, panel a, for one monomeric subunit. When the six insulin monomers undergo the T- to R-transition to form the R_6 hexamer, the six helices form six amphiphilic pockets, which bind phenol molecules (*3*). A phenol molecule is drawn in Figure 2B, panel a, to indicate the location of the phenol-binding pocket which is situated between the two short helices of the A chain. In the R_6 hexamer, the conformation of insulin imposes a tetrahedral coordination to the zinc site, as shown in Figure 2B, panel b. The ligands are the same three nitrogens from HisB10 residues, and the fourth ligand is phenoxide or another exogenous ligand. In terms of zinc binding, the hexamer is better viewed as a dimer of trimers located on opposite sides of the cylindrical hexamer. Each trimer is formed by three equivalent monomers related by the 3-fold axis of symmetry. Panel C of Figure 2 provides a top view, along the 3-fold axis of symmetry, of the upper

[1] Abbreviations: NMR, nuclear magnetic resonance; NOESY, nuclear Overhausser effect spectroscopy; Terpy, 2,2′,2″-terpyridine; DSS, 2,2-dimethyl-2-silapentane-5-sufonate-2,2,3,3,-d4; Tris, tris[hydroxymethyl]amino methane; LFSE, ligand field stabilization energy; LFAE, ligand field activation energy.

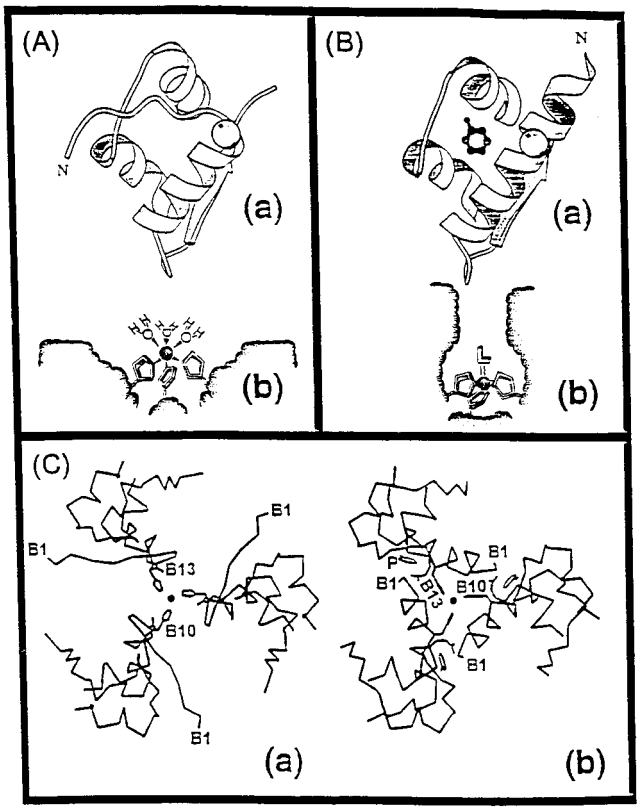

FIGURE 2: Diagrams showing differences between monomeric subunits of the T_6 hexamer (A,a) and R_6 hexamer (B,a) and the coordination geometry of the zinc site, which is octahedral in the T_6 (A,b) and tetrahedral in the R_6 hexamer (B,b). The phenol-binding pocket is located between the two short helices of the A chain as indicated in (B,a). Panel C shows a top view of the upper trimers down the 3-fold axis of symmetry of the T_6 (a) and the R_6 (b) insulin hexamers. Redrawn with permission from ref *31*.

trimers of the T_6 (a) and the R_6 (b) hexamer. This view shows one zinc-binding site and the side chains of residues HisB10 and GluB13. A phenol molecule (P) is also shown bound in the R_3 trimer (Figure 2C, panel b). The T_6 to R_6 transition occurs via an intermediate asymmetric T_3R_3 (*4, 5*) or $T_3R_3^f$ (*6, 7*) hexamer, composed of one T_3 trimer and one R_3 trimer. In the $T_3R_3^f$, the B chain is α-helical from residue B3 to B19 and tetrahedral coordination has been observed in its T_3 trimer (*7*). For simplicity of notation, hereafter, we use T_3R_3 to represent the asymmetric hexamer, although a T_3R_3 hexamer with the B chain α-helical from residue B1 to B19 has never been observed in crystalline state (*7*). NMR studies indicate that asymmetry within the dimers of the R_6 hexamer is removed in solution (*4*). The T- to R-transition has been extensively studied both in crystalline state (*3, 6*−*10*) and in solution (*4, 5, 11*−*34*). It is now well established that the insulin hexamer is an allosteric protein that is stabilized by both homotropic interactions between the phenol-binding pockets and heterotropic interactions between the phenol-binding pocket and the zinc-binding site (*4, 26, 29, 30*).

The zinc sites of the 2-zinc−insulin hexamer are known to accommodate a number of divalent metal ions such as Cd^{2+}, Co^{2+}, Cu^{2+}, Ni^{2+}, Fe^{2+}, and Mn^{2+} (*35*). In solution, the T- to R-transition has been well documented for the native zinc(II)−insulin hexamer (*4, 20, 29*), the cobalt(II)- (*5, 21, 24*), and the copper(II)- and the copper(I) (*27, 28*)-substituted insulin hexamers. A zinc-free R_6 hexamer has been reported to exist in solution (*36*), and evidence for an R-state tetramer has been presented (*37*). A zinc-free $T_3R_3^f$ hexamer has been observed in crystalline state with the B13 Gln mutant (*8*). The literature reports that when nickel(II) is placed in the zinc site, the T- to R-conformation transition is impeded (*17*). The latter report implies a role of the metal ion in the T- to R-transition, whereby the nature of the metal ion in the HisB10 site modulates the energetic barrier(s) during the T- to R-state transition. Herein we report evidence indicating that, under suitable conditions, Cd(II)-, Ni(II)-, and Fe(II)/(III)-substituted insulin hexamers all are capable of forming R-state species. Effects of the metal ions on the rate of dissociation of the hexamer provide evidence for the role of ligand field stabilization effects, Lewis acidity effects, and coordination geometry preference in the allosteric T- to R-state transition. We also report ^{113}Cd NMR evidence for the alteration of the calcium binding site upon the T- to R-transition. This finding is an added consideration in the formulation of the allosteric transition mechanism.

MATERIALS AND METHODS

Materials. Metal-free human insulin and the HisB10 → Asp mutant were gifts from Novo-Nordisk (Bagsvaerd, Denmark). Nickel sulfate ($NiSO_4$), iron(II) ammonium sulfate [$Fe(NH_4)_2(SO_4)_2$], 2,2′,2″-terpyridine (Terpy), imidazole, tris-[hydroxymethyl]amino methane (Tris) and phenol-d_6 were purchased from Sigma. Cadmium sulfate ($CdSO_4$) was purchased from J. T. Baker Chemical Co. Copper sulfate ($CuSO_4$) was purchased from Allied Chemical. Potassium thiocyanate (KSCN) was purchased from Mallinckrodt. Sodium chloride (NaCl) was purchased from Fisher Scientific Co. Deuterated water (D_2O), Sodium deuterioxide (NaOD), imidazole-d_4, and 2,2-dimethyl-2-silapentane-5-sulfonate-2,2,3,3,-d_4 (DSS) were purchased from Aldrich Chemical Co.

Sample Preparation. Insulin concentrations were determined from the absorbance at 280 nm by using the extinction coefficient $\epsilon_{280nm} = 5.7 \times 10^3\ M^{-1}\ cm^{-1}$ (*38*). Concentrations of metal ions were determined via spectrophotometric titration of their complexes with Terpy. The bis complex extinction coefficients are as follows ($M^{-1}\ cm^{-1}$): Zn-(Terpy)$_2$, $\epsilon_{333nm} = 4.10 \times 10^4$; Cd(Terpy)$_2$, $\epsilon_{330nm} = 3.25 \times 10^4$; Ni(Terpy)$_2$, $\epsilon_{334nm} = 3.2 \times 10^4$; and Fe(Terpy)$_2$, $\epsilon_{550nm} = 1.13 \times 10^4$ (*39*).

NMR Measurements. ^{1}H NMR spectra were recorded at 500 MHz on a G. N. NMR spectrometer at a probe temperature of 26 ± 1 °C. Chemical shifts are reported relative to the resonance due to DSS.

Kinetic Measurements. Single-wavelength rapid-kinetic measurements were performed with a Durrum stopped-flow apparatus and computerized data acquisition system as described by Dunn et al. (*40*). The absorbance versus time data were fitted to a sum of exponential functions, employing the minimum number of phases necessary to reconstruct the experimental time course without systematic deviation. All kinetic experiments were carried out in 0.05 M Tris-$HClO_4$ buffer, pH 8.0.

RESULTS

(1) ^{1}H NMR Signatures of the R-State for Cd(II), Ni(II), and Fe(II)/Fe(III) Substituted Insulin Hexamers. The ^{1}H NMR signatures of R-state insulin hexamers containing the metal ions Zn(II), Co(II), Cu(I), and Cu(II) have been

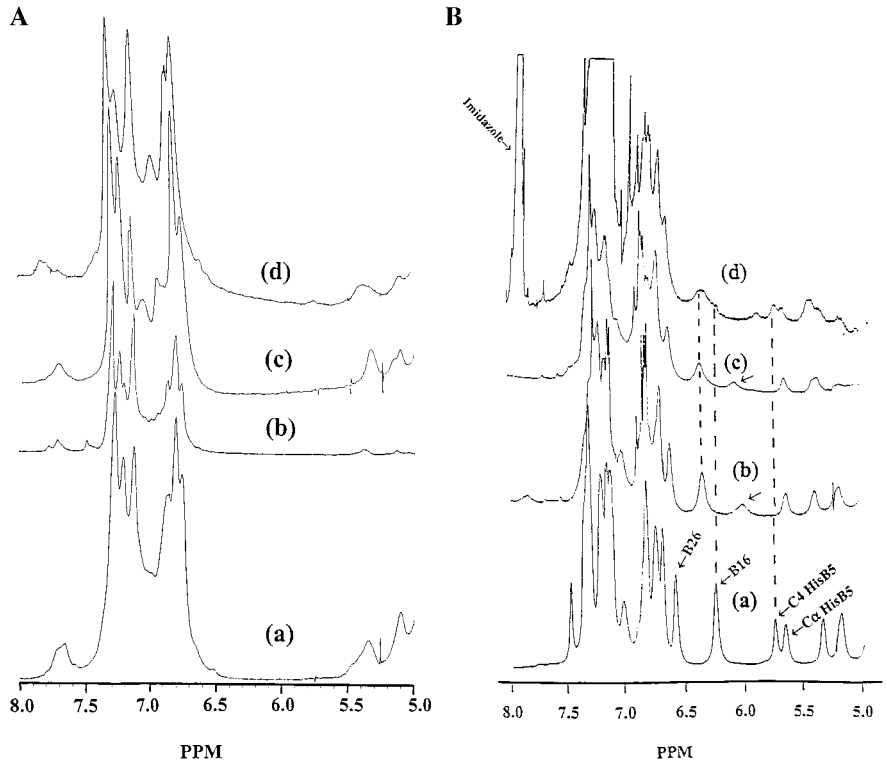

FIGURE 3: (A) Aromatic region of the ^{1}H NMR spectra of T-state metal ion-substituted insulin hexamers for (a) Zn(II), (b) Cd(II), (c) Ni(II), and (d) Fe(II), in D_2O at pH 8.0 (meter reading). The concentration of insulin is 2 mM (monomeric subunit) and the concentrations of metal ions is 1 mM. (B) Aromatic region of the ^{1}H NMR spectra of metal-ion-substituted insulin hexamers under the following conditions: (a) 0.10 M phenol and 0.10 M NaCl for Zn(II), (b) 0.10 M phenol for Cd(II), (c) 0.01 M phenol for Ni(II), and (d) 0.10 M phenol + 0.10 M imidazole for Fe(III). Prominent R-state signatures include the resonances which arise between 6.5 and 5.5 ppm. The concentration of insulin is 2 mM (monomeric subunit), and the concentration of metal ions 1 mM. Arrows in spectra b and c point to the resonance assigned to C4 HisB5 proton in the Cd(II)- and Ni(II)-T_3R_3 insulin hexamers.

reported previously (*4, 12, 16, 21, 24, 27*). They consist of specific resonances which arise in the aromatic region of the spectrum upon the T- to R-transition. In the absence of phenol and lyotropic anions, the T-state is predominant. The aromatic regions of the ^{1}H NMR spectra of the Zn(II), Cd-(II), Ni(II), and Fe(II) insulin hexamers under T-state conditions are shown in Figure 3A. A broad, featureless envelope of overlapping resonances characterizes the spectral region from 7.4 to 6.5 ppm. Resonances in the latter region are due to aromatic ring protons of four tyrosine residues (TyrA14, TyrA19, TyrB16, and TyrB26), three phenylanine residues (PheB1, PheB24, and PheB25), and the C4 protons of HisB5 and HisB10 (27). The C2 protons of HisB10 and His B5 resonate between 7.4 and 8.0 ppm (*13, 18*). The absence of resonances between 6.5 and 5.5 ppm is characteristic of all spectra of insulin hexamers under T-state conditions (*4, 13, 18, 21, 27*). Figure 3B shows the spectra of the Zn(II)−insulin hexamer in the presence of 0.10 M phenol and 50 mM chloride (a), the Cd(II)-substituted insulin hexamer in the presence of 0.10 M phenol (b), the Ni(II)-substituted insulin hexamer in the presence of 0.10M phenol, (c) and the Fe(III)-substituted insulin hexamer in the presence of 0.10 M phenol and 0.10 M imidazole (d). Under these conditions, resonances arise between 6.5 and 5.5 ppm for all the metal ions and resonances between 7.4 and 6.5 ppm become sharper. Resonances due to C2 protons of HisB5 and HisB10 have also been shifted from the spectral region between 7.4 and 8.0 ppm. For the Zn(II)−insulin hexamer, resonances are observed at chemical shifts of 6.30, 5.80, and 5.65 ppm (spectrum a in Figure 3B) which have been assigned previously by Brzovic (*4*) to 3,5 protons of TyrB16, C4 proton of His B5, and Cα proton of HisB5, respectively, in the Zn(II)-R_6 hexamer. The shifts undergone by the latter resonances can all be justified by interactions observed in the crystalline state (*4*, section 1 of the Discussion). In the case of Cd(II)- and Ni(II)-substituted insulin hexamers (spectra b and c in Figure 3B), a broad resonance is observed at ∼6.0 ppm (an arrow points to this resonance), instead of the sharp resonance due to C4 proton of His B5 observed at 5.8 ppm for the Zn(II)-R_6 hexamer (Figure 3B, panel a) (*4*). We attribute the broad resonance at ∼6.0 ppm to the C4 proton of HisB5 in T_3R_3 hexamers (see section 1 of the Discussion for justification).

An additional signature of the R-state results from the interaction of HisB5 and TyrB16 side chains from adjacent subunits across the monomer−monomer interface, where they make van der Waals contacts in the R_6 hexamer (*9*). In the ^{1}H NMR spectrum, this interaction is manifested in the form of a nuclear Overhauser effect between the C2 proton of HisB5 and the 2,6 ring protons of TyrB16 (*37*). Figure 4 shows the aromatic portion of the NOESY spectrum of the Cd(II)-substituted HisB10 → AspB10 insulin hexamer in the presence of phenol. In the mutant complex, only one resonance occurs between 8.0 and 7.4 ppm. This resonance is due to the C2 proton of HisB5, the only histidine residue in the mutant. The NOESY spectrum shows that the resonance due to the C2 proton of HisB5 is correlated to a resonance at 7.32 ppm. The latter resonance has been assigned previously to the 2,6 ring protons of TyrB16 (*37*). The rings of residues HisB5 and TyrB16 make van der Waals

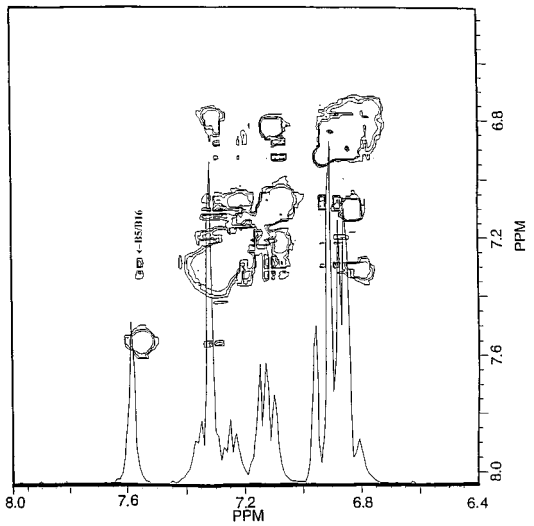

FIGURE 4: Aromatic region of a 2D NOESY spectrum of the Cd(II)-B10Asp insulin hexamer in D_2O. Notice the cross-peak between a singlet at 7.55 ppm (resonance due to the C2 proton of HisB5) and a doublet at 7.35 ppm (due to the 2,6 ring protons of TyrB16). The concentration of the insulin mutant is 2 mM and the concentration of Cd(II) is 1 mM. Phenol (100 mM) is used to induce the R-state as per previous experiments (Figure 3B). The pH is 9.4 (meter reading).

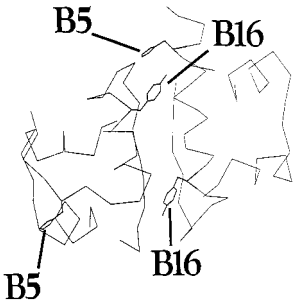

FIGURE 5: Graphics-generated structure showing the rings of tyrosine B16 and histidine B5 in the R-state (top) and in the T-state (bottom) at the monomer-monomer interface of the insulin hexamer. In the R_6 and the T_3R_3 hexamers, the two rings are located within the van der Waals distances.

contacts in the R_6 and T_3R_3 conformation states (Figure 5, top) but never in the T_6 hexamer (Figure 5, bottom). We therefore conclude that cross-peak a between the resonance due to the C2 proton of HisB5 and the resonance due to the 2,6 ring protons of TyrB16 is a signature of the R-state conformation. It is worthwhile to mention here that the HisB10 → Asp mutant does not form the hexamer in the presence of Zn(II) (*41*). However, according to our ^{113}Cd NMR experiments, it combines with Cd(II) in the ratio of six monomers to three Cd(II) to form the hexamer (data not shown). In the ^{113}Cd NMR spectrum of the $(Cd^{2+})_3$(HisB10 → Asp)$_6$, no signal due to free Cd(II) is observed at 0 ppm. The inclusion of three Cd(II) in the hexamer suggests that the aspartate side chains form two Cd(II)-binding sites and that the third Cd(II) is bound in the known GluB13 binding site illustrated in Figure 1 (*2*).

(2) Kinetics Measurements. Kinetic measurements were performed to compare the rate of displacement of metal ions from the R-state and the T-state insulin using the chelator terpyridine. Terpyridine forms complexes with all transition metal ions that exhibit high molar absorptivity around 320 nm ($\epsilon \approx 10^4$ M^{-1} cm^{-1}). Due to the wide variation in observed rates, it was necessary to use both stopped-flow and standard manual addition techniques. Kinetic experiments were conducted under three experimental conditions: (a) conditions that favor the formation of the Zn(II)-T_6 hexamer (in the absence of exogenous ligand) (*31*), (b) conditions that favor formation of the Zn(II)-T_3R_3 hexamer (0.20 M KSCN) (*4*), and (c) conditions that favor the formation of the Zn(II)-R_6 hexamer (0.10 M phenol plus 0.10 M NaCl) (*4*). Reactions were conducted in the presence of an excess of terpyridine (400 μM) relative to the hexamer (3.75 μM). All kinetic traces could be fitted with two exponential functions representing two apparent pseudo-first-order events. Figure 6 shows a typical fitted kinetic trace and the residuals. The relative standard errors on the estimated parameters were typically 1% or less. Table 1 lists the pseudo-first-order rate constants for the first and the second phase of the reaction under T_6 conditions (T_1, T_2), under T_3R_3 conditions (TR_1, TR_2) and under R_6 conditions (R_1, R_2).

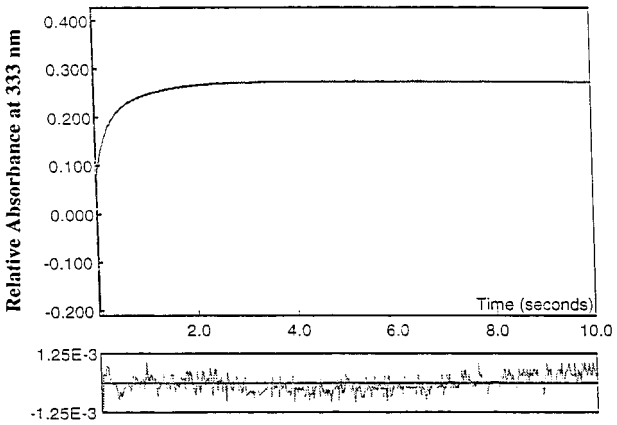

FIGURE 6: Typical time course trace for the reaction of terpyridine with the metal ion-substituted insulin hexamer. Data shown are from the reaction of the zinc−insulin hexamer under T-state conditions. The calculated curve superimposed on the experimental data is a sum of two exponential functions. Residuals from the fit are displayed in the bottom box.

Under conditions which favor the T-state, for metal ions with partially filled d subshells, the rate constant of the first and second phase follow the order Co(II) > Cu(II) > Ni(II). For the two metal ions with completely filled d subshells, the rate of the first phase is much higher for the reaction of terpyridine with the Cd(II)−insulin hexamer than that with the Zn(II)−insulin hexamer. The rate constant for the second phase is somewhat higher for Zn(II) (0.710 s^{-1}) than for Cd(II) (0.620 s^{-1}). Under conditions which favor the formation of the Zn(II)-R_6 hexamer, the rate of the first phase detected follows the order Co(II) > Ni(II) > Cu(II). The rates for the second phase increase in the order Ni(II) < Cu(II) < Co(II). Under Zn(II)-R_6 conditions, the rates of the first and second phases are faster for the Cd(II)−insulin hexamer than for the Zn(II)−insulin hexamer. Under conditions favoring formation of the Zn(II)-T_3R_3 hexamer, the rate of the first and second phase increase in the order Ni(II) < Cu(II) < Co(II). Under these conditions, the Cd(II)−insulin hexamer reacts a lot slower than the Zn(II)−insulin hexamer.

(3) UV−Vis Signatures of the R-State. Only the iron(II)/(III)-substituted insulin hexamer system produced useful

Table 1: Rate Constants (s^{-1}) for the First and Second Phase during Dissociation of Metal Ion-Insulin Hexamers under T-State Condition, in the Absence of Ligand [$k(T_1)$, $k(T_2)$]; under R-state Conditions, in the Presence of 0.10 M Phenol and 0.10 M NaCl [$k(R_1)$, $k(R_2)$] and under Conditions that Favor Formation of the Zn(II)-T_3R_3 Hexamer, in the Presence of 0.20 M KSCN [$k(TR_1)$, $k(TR_2)$][a]

metal ion	$k(T_1)$	$k(T_2)$	$k(R_1)$	$k(R_2)$	$k(TR_1)$	$k(TR_2)$
Co(II)	2.30×10^1	7.80×10^{-1}	2.20	2.30×10^{-1}	1.72×10^2	1.10×10^1
Cu(II)	2.10	3.20×10^{-1}	2.10×10^{-2}	1.50×10^{-2}	3.80	2.90×10^{-1}
Ni(II)	5.70×10^{-1}	4.00×10^{-2}	1.30×10^{-1}	1.60×10^{-3}	2.20	6.00×10^{-2}
Zn(II)	3.40	7.10×10^{-1}	2.90×10^{-2}	9.60×10^{-4}	5.20×10^{-1}	4.90×10^{-2}
Cd(II)	1.90×10^1	6.20×10^{-1}	3.30×10^{-1}	1.00×10^{-2}	5.50×10^{-2}	slow

[a] Experimental conditions: final concentrations of metal ions, insulin monomer, terpyridine, chloride, phenol and thiocyanate were 7.5 μM, 37.5 μM, 400 μM, 100 mM, 100 mM, and 200 mM, respectively. The solvent was 0.05M Tris-ClO_4 buffer at pH 8.0.

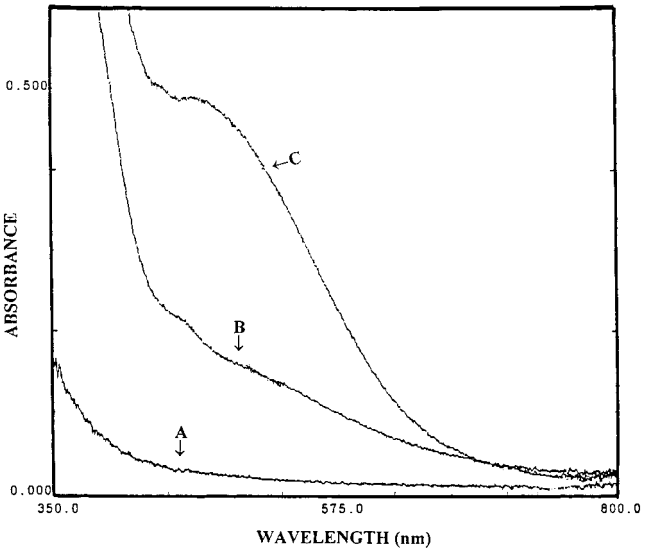

FIGURE 7: Progressive changes in the UV−vis spectrum of Fe(II)−insulin hexamer (0.33 mM hexamer) from T-state conditions (A), after addition of phenol (B), and after addition of phenol and imidazole (C). The most significant change in the spectrum occurs upon addition of imidazole; the molar absorptivities strongly increase between 440 and 600 nm.

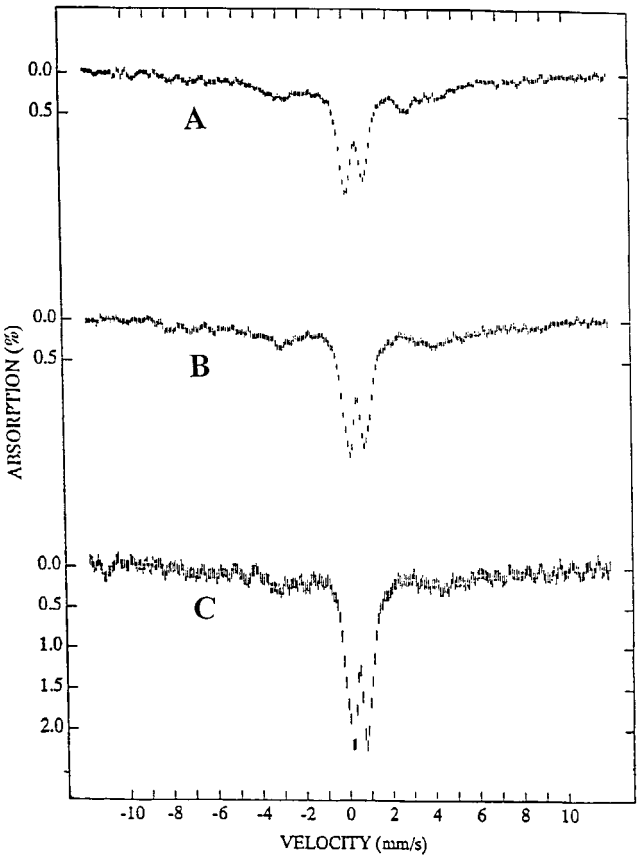

FIGURE 8: Mössbauer spectra of the Fe(III)−insulin hexamer in the presence of 0.100 M phenol (A), in the presence of 0.100 M phenol and 0.100 M imidazole (B and C). The ratio of Fe(III) to insulin is 3:6 in panels A and C and 2:6 in panel B. The concentration of Fe(III) is 1.5 mM and the pH 8.

electronic spectra. Figure 7 shows the progression in the spectrum from T-state conditions (in the absence of phenol or other exogenous ligands) (A), after addition of phenol (B), and after addition of phenol and imidazole (C). Under T-state conditions, radiation between 400 and 600 nm is only weakly absorbed. When phenol is added, the absorbance between 400 and 600 nm remains low. When imidazole is added in the presence of phenol, a strong absorbance band centered at 480 nm arises in the electronic spectrum (Figure 7C). The extinction coefficient calculated ($\epsilon \approx 500$ M^{-1} cm^{-1}) suggests that this band is a charge-transfer (CT) band. Electron paramagnetic resonance (EPR) and Mössbauer spectra of the phenoxide complex are consistent with 100% occupation of the zinc sites by high-spin Fe(III). Figure 8 shows Mössbauer spectra of the Fe(III)−insulin hexamer in the presence of phenol (A) and in the presence of phenol and imidazole (B and C). The isomer shift in the three spectra is 0.5 mm/s, which is typical of ferric high-spin centers. An isomer shift of 1.42 mm/s was measured for the reference ^{57}Fe(II) sample. The Mössbaeur spectrum is sharpest and cleanest when the ratio of Fe^{3+} to insulin monomers is 3:6 (spectrum C in Figure 8).

(4) ^{113}Cd NMR Evidence of the Alteration of the Calcium Site. Figure 9, panels A and B, presents ^{113}Cd NMR spectra of the $(Cd^{2+})_3(insulin)_6$ hexamer in the absence and the presence of phenol, respectively. In the absence of phenol, two resonances are detected at −34.5 and 150 ppm, which have been previously assigned to Cd(II) in the calcium site and Cd(II) in the two zinc sites, respectively (*2*). These chemical shifts are consistent with known effects of oxygen and nitrogen ligands on the ^{113}Cd chemical shift (*42*, and references therein). Upon addition of phenol to the hexamer, the resonance due to cadmium bound by the GluB13 carboxylates is lost (Figure 9B).

DISCUSSION

Using characteristic ^{1}H NMR signatures due to protons of amino acid residues in insulin, we have demonstrated in this paper that Cd(II)-, Ni(II)-, and Fe(II)/(III)-substituted insulin hexamers all undergo the T- to R-conformational change. However, direct and unambiguous evidence of the change of the metal ion HisB10 sites from octahedral

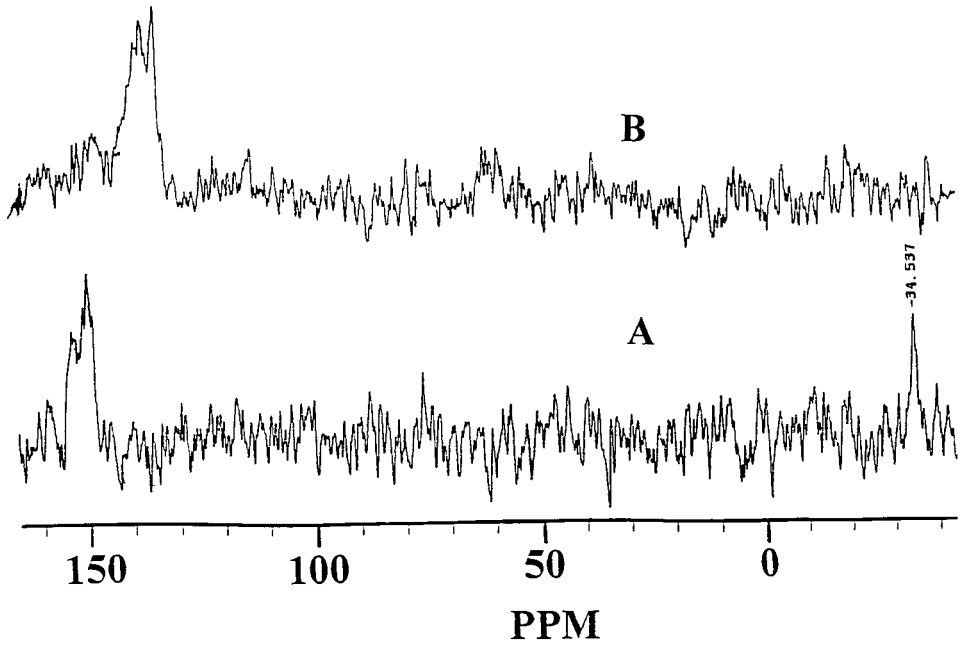

FIGURE 9: Spectra of the $(Cd^{2+})_3$(insulin)$_6$ hexamer in the absence (A) and the presence (B) of phenol, respectively. In the absence of phenol, two resonances are detected at −34.5 and 150 ppm which have been previously assigned to Cd(II) in the calcium site and Cd(II) in the two zinc sites, respectively (Sudmeir et al., 1981). The calcium site is located at the center of the hexamer and is formed by the six carboxylates from the six GluB13 residues as shown in Figure 1. Upon addition of phenol to the hexamer, the resonance due to cadmium bound in by the GluB13 carboxylates is lost.

geometry in the T-state to tetrahedral geometry in the R-state has not yet been obtained. Because the major conformational change (B1−B8 extended chain to helix) on the six subunits significantly alters the topology of the hexamer, including the environments of the HisB10 zinc sites, a change in coordination is more likely than not. These metal-ion-substituted insulin hexamers provide new probes for the investigation of the role of the metal ion in the T- to R-allosteric transition in the insulin hexamer. These hexamers may also serve as models for the metal ion sites in other metalloproteins.

(1) Cd(II) and Ni(II) Form Predominantly T_3R_3 Hexamers in the Presence of Phenol. The changes observed from panel A to panel B in Figure 3 provide strong evidence that a T- to R-state transformation has taken place for all the metal-ion-substituted insulin hexamers. The differences in the chemical shifts of R-state signatures between 6.5 and 5.5 ppm of the Zn(II)-R_6-Cl hexamer and the other metal ion-substituted hexamers is an indication that the equilibrium is not totally shifted toward the formation of R_6 hexamers under the conditions used. The R-state is stabilized by homotropic interactions among the phenol-binding pockets and heterotropic interactions between the phenol-binding pockets and the zinc-binding site (*4*, *29*). Suitable ligands for coordination to the zinc-binding site are required for shifting the equilibrium in favor of the R_6 hexamer. Chloride fulfills this role for the Zn(II)−insulin hexamer but does not for the Cd(II)- and the Ni(II)-substituted insulin hexamers. A search for effective heterotropic effectors for the Ni(II)- and the Cd-(II)-substituted hexamers is in progress. Careful examination of the spectra of the Cd(II)−insulin and Ni(II)−insulin hexamers in the presence of phenol suggests that the predominant species under our experimental conditions is the T_3R_3. In fact, the two spectra (b and c in Figure 3B) bear a striking resemblance to a spectrum attributed to T_3R_3 during titration of the Zn(II)−insulin hexamer by phenol in the presence of 50 mM NaCl (*4*). The resonance due to the C4 proton of His B5 is a very sensitive probe of the binding of phenol in the phenol pocket. Formation of the B1−B8 helix brings the HisB5 residue in van der Waals contact with the phenol ring in the R-state and a hydrogen bond is produced between the carbonyl oxygen of His B5 and the hydroxyl of TyrB16 (*9*). It has been demonstrated that ring currents in the phenol ring shifts the resonance frequency of the C4 proton of His B5 proton upfield to ∼5.8 ppm (*4*) in the Zn(II)-R_6 hexamer. However, during the titration, at 1.5 mM concentration of phenol, a broad resonance is observed at 6.0 ppm, exactly the same chemical shift of the broad resonance observed in the spectra of the Cd(II)- and Ni(II)-substituted hexamers in the presence of 0.10 M phenol (Figure 3B, spectra b and c). In the case of the Zn(II)−insulin hexamer, as the concentration of phenol increased to 20 mM, all spectral changes are saturated and the broad resonance at 6.0 ppm is shifted upfield to 5.8 ppm and becomes sharper (labeled C4His B5 in Figure 3B, panel a). Careful interpretation of spectral changes during the titration assigns the appearance of the spectrum obtained at 1.5 mM phenol to the T_3R_3 hexamer (*4*). Due to expected paramagnetic effects of the unpaired electrons of the Fe(III) center on the width and shifts of resonances in its proximity, similar analysis of the Fe(III)−insulin spectrum may lead to erroneous conclusions.

(2) Heterotropic Interactions Stabilize the R-State Conformation in the Fe(III)-Substituted Insulin Hexamer. Oxidation of Fe(II) to Fe(III) does not prevent the T- to R-allosteric transition. ^{1}H NMR R-state signatures are elicited by addition of an appropriate ligand, imidazole (compare panel d of Figure 3A and panel d of Figure 3B). This behavior parallels that of the Cu(II)-substituted insulin hexamer in which heterotropic interactions between the phenol-binding pocket and ligand binding to Cu(II) are necessary to stabilize the R-state (*26*−*28*). It seems, therefore, that heterotropic

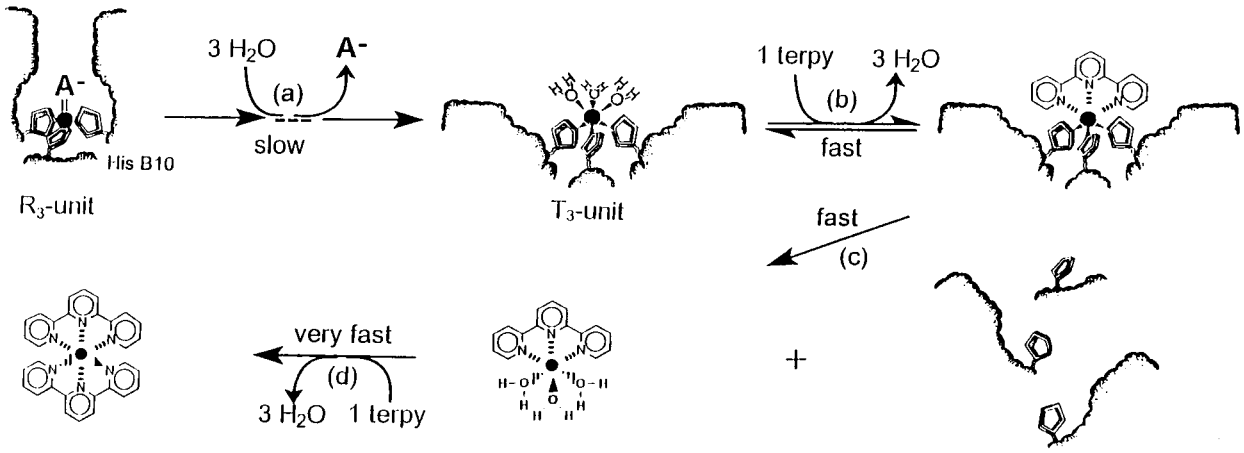

FIGURE 10: Kinetic scheme for the terpyridine-induced dissociation of the metal−insulin complex. (a) conformational transition between the R_3 and the T_3 units and change of coordination geometry from tetrahedral to octahedral. (b) Coordination of one terpyridine molecule to the T_3 trimer-bound metal ion. (c) Dissociation of the M(terpyridine)$_1$ monocomplex. (d) Coordination of a second terpyridine molecule to the M(terpyridine)$_1$ monocomplex. Anionic ligands for the HisB10 site are designated with A^-, and the metal site is designated (●). Reproduced with permission from ref *34*.

interactions also are operative in the Fe(III)-substituted insulin hexamer. Effects of several ligands on the electronic spectrum were investigated. According to UV−visible effects, only ligands containing nitrogen atoms available for coordination are effective allosteric effectors of the Fe(III)-substituted hexamer. It is possible that the absorbance band (a charge-transfer band) elicited by addition of imidazole expresses the phenol-induced change in coordination geometry from octahedral to tetrahedral as it occurs when the metal ion is Zn(II) (*3*), Co(II) (*24*), and Cu(II) (*27, 28*). The Fe(III)-substituted insulin hexamer can be viewed as a non-heme iron protein. The possibility of tetrahedral coordination to four nitrogens upon formation of the R-state raises interesting questions about the coordination chemistry of Fe(III) in proteins. The known iron proteins with tetrahedrally coordinated iron are mainly sulfur−iron cluster proteins such as Rubredoxin and Ferrodoxin (*43*). Tetrahedral coordination of Fe(III) with ligation to four nitrogens has never been reported for a non-heme iron-binding protein. If tetrahedral geometry is indeed attained in the R-state Fe(III)−insulin hexamer, then it represents a unique case of iron coordination chemistry in a protein. Note, however, that, in the case of the insulin hexamer, the possibility of a trigonal bipyramidal geometry is not to be excluded.

(3) Cd(II) Experiences Weak Binding in an R-State Altered Calcium-Binding Site. The disappearance of the resonance due to Cd(II) in the putative calcium site suggests that the calcium site is at minimum altered if not obliterated. Crystalline state studies show that in the T_6 hexamer the six GluB13 side chains form an ordered hydrogen-bonded network (*1*). The latter network is disrupted in the T_3 R_3^f (*7*) and in the R_6 (*8*) hexamers, and the conformation of the GluB13 side chains is very much dependent on the hexamer type (*7*). The present study suggests that upon the T- to R-state transition in solution, GluB13 undergoes conformational changes similar to those observed in crystalline state and that this change has a significant effect on the binding in the calcium site. Because the disappearance of the Cd(II) signal at −34.5 ppm is not accompanied by the appearance of a resonance due to free Cd(II) at 0 ppm, the displaced Cd(II) must be involved in exchange between sites. This assumes that at least two species exist in equilibrium, and exchange between them takes place at a rate that precludes observation of the signal(s) (*42*). Therefore, we propose that Cd(II) still binds, albeit weakly in the altered putative calcium-binding site.

(4) Effects of Metal Ions on the Rate of Dissociation of the Insulin Hexamer. (a) Mechanism of the Terpyridine-Induced Dissociation of Insulin Hexamers (Figure 10). Detailed studies of the concentration effects and allosteric ligands effects on the rates of displacement of Zn(II) by terpyridine from the insulin hexamer have been conducted (*20, 34*). The mechanism proposed for the dissociation of the R_6, T_3R_3, and T_6 hexamer is depicted in Figure 10 to facilitate the reading of interpretations and arguments which rely on it. Under T_6 conditions, two T_3 trimers are the reacting species. The mechanism proposed to account for the two relaxations consists of a fast coordination of the chelator to the protein-bound zinc ion (step b in Figure 10), followed by the rate-limiting dissociation of the chelator-bound zinc ion from the protein (step c in Figure 10) and the rapid coordination of a second chelator molecule to give the bis complex (step d in Figure 10). When R_3 trimers are the reacting species, the rate-limiting step becomes the conversion of the R_3 to a T_3 trimer (step a in Figure 10) (*20, 34*). This conversion is required because access to the fourth ligand on the tetrahedral zinc site is via a narrow tunnel 12 Å long (*6, 7*) that is too small to accommodate the bulky terpyridine. The decrease in the rate of displacement of Zn(II) from the insulin hexamer from $T_6 > T_3R_3 > R_6$ has been interpreted as due to the relative inaccessibility of the metal site in the R-state (*20, 34*).

(b) Ligand Field Stabilization Energy (LFSE) Effects Determine the Relative Activation Energy for the Dissociation of the T6 Hexamers. In the T_3 octahedral field, Ni^{2+} is expected to have the largest LFSE, which leads to high ligand field activation energy (LFAE) and the consequent slower displacement of the Ni(II) (*45*). In octahedral complexes, the principal factor determining the activation energy for the replacement of a ligand is the breaking of the bond between the metal and the leaving group (*46*). In the case of the T_6 hexamer, the first phase of the reaction involves three water molecules leaving groups (step b in Figure 10) and the second phase of the reaction involves three imidazolyl side chains

of HisB10 residues' leaving groups (step c in Figure 10). The first phase of the reaction of terpyridine is slowest for the Ni(II)-substituted hexamer, which reflects considerable stabilization of the Ni(II)−H_2O bonds compared to Co(II)−H_2O and Cu(II)−H_2O. Similarly, the slow second phase of the reaction of the Ni(II)−insulin complex reflects stabilization of the Ni(II)-imidazolyl bond by the high LFSE of Ni^{2+}. Although Cu^{2+} has lower LFSE than Co^{2+} in both weak and strong octahedral ligand field (*46*), the Co(II)−insulin hexamer reacts approximately two times faster than the Cu(II)−insulin hexamer. This behavior can be accounted for by Jahn−Teller effects operative in Cu^{2+}. With its d^9 electronic configuration, Cu^{2+} possesses a degenerate ground-state electronic configuration. Coordination geometries of d^9 metal ion complexes such as Cu^{2+} are known to be irregular due to distortions, which occur to remove degeneracy. Jahn−Teller distortions enhance the strength of the four bonds in the plane, while the remaining axial positions are more weakened (*44*).

The Cd(II)−H_2O bonds are expected to be weaker than the Zn(II)−H_2O bonds as a result of the larger radius of Cd(II). Thus, the faster first phase for reaction of the Cd(II)−insulin hexamer is consistent with a lower activation energy due the weaker Cd(II)−H_2O bond. The rate of the second step is somewhat higher for Zn(II) ($k = 0.710\ s^{-1}$) than for Cd(II) ($k = 0.620\ s^{-1}$). This result indicates that the activation energy for the reaction of intermediate terpyridine−Cd−insulin complex is slightly higher than that of the Zn(II) analogue, meaning that the intermediate ternary insulin−Cd(II)−terpyridine complex lies lower in energy than the insulin−Zn(II)−terpyridine complex. We propose that the higher stability of the ternary insulin−Cd(II)−terpyridine as compared to the insulin−Zn(II)−terpyrine complex reflects the ability of the larger size Cd(II) to accommodate the bulky terpyridine better than Zn(II).

(c) Preference for Coordination Geometry Determines the Activation Energy of the R_3 to T_3 Transition. Under conditions favoring the formation of the Zn(II)-R_6 hexamer, the relative rates of the first phase detected [Co(II) > Ni(II) > Cu(II)] cannot be justified by LFSE effect. However, they can be rationalized in terms of the requirement for a change in coordination geometry from tetrahedral to octahedral upon the R_3 to T_3 conversion (step a in Figure 10) (*34*). According to our results, the activation energy for this conversion depends on the nature of metal ion and increases in the order Co(II) < Ni(II) < Cu(II). We propose that this order suggests a correlation between the activation energies and the relative preference of the metal ions for tetrahedral versus octahedral geometry. Due its d^7 electronic configuration, ligand field stabilization energies disfavor the tetrahedral configuration in Co(II) relative to the octahedral one to a smaller extent than any other d^n ($1 \leq n \leq 9$) configuration. Accordingly, the activation energy for the conversion of Co(II)-R_3 to Co(II)-T_3 is the lowest as indicated by the highest rate constant compared to the other transition metal ions. When a Co(II) site in a protein is accessible to ligands from solution, such as in Co(II)-carbonic anhydrase, Co(II)-carboxypeptidase, and Co(II) alkaline phosphatase, Co(II) displays a propensity for the formation of five-coordinate adducts (*47*). In contrast, Cu(II) displays a preference for tetrahedral coordination geometry in the insulin hexamer ligand field (*28*). During the formation of Cu(II) complexes, addition of the sixth ligand is highly unfavorable and even the fifth ligand is only weakly bound due to the Jahn−Teller effect (*44*). Our results indicate that the formation of the intermediate, which must be tetragonally distorted octahedral Cu(II), requires a higher activation energy then the formation of the intermediate distorted octahedral Co(II) and Ni(II) complexes. Presumably, the intermediate Cu(II)-T_6 is of high energy due to the two weak trans bonds.

The rates for the second phase, attributed to steps b and c in Figure 10 (*34*), increase in the order Ni(II) < Cu(II) < Co(II), consistent with LFSE effects and stabilization of the Cu^{2+} complex by Jahn−Teller distortions. The latter order is therefore consistent with the reaction of terpyridine with the T_3 trimers (step b in Figure 10). The relative activation energies for the second step of the reaction of these transition metal ion−insulin hexamers thus excludes the possibility that terpyridine reacts directly on the R_3 trimer.

The first phase involving the R_3 to T_3 transition is 11.4 times faster for the Cd(II)− than for Zn(II)−insulin hexamer, suggesting that Cd(II) is more accommodating of octahedral ligand field than Zn(II). This effect is consistent with the larger size of Cd(II), which accommodates six ligands better. The second phase involving the breaking of metal ions−insulin bonds is also faster for Cd(II) than for Zn(II) consistent with weaker Cd−N bonds. We conclude, therefore, that the rapid rate of dissociation of the Cd(II)-substituted insulin hexamer and the slower rate of dissociation of the Zn(II)-substituted insulin hexamer reflect the relative thermodynamic stability of the metal ion−insulin bonds. This is in agreement with recent kinetic studies (*34*).

(d) Evidence for the Influence of the Lewis Basicity of the Exogenous Ligand on the Activation Energy of the Dissociation of the Hexamer. In the presence of KSCN, the first phase is attributed to the reaction of the T_3 trimer and the second phase to the reaction of the R_3 trimer (*34*). When the reaction of the T_3 trimers under thiocyanate conditions is compared to the reaction of the T_3 trimers in the T_6 hexamers, the most dramatic effect is observed for the Cd(II)−insulin hexamer. The first phase due to the reaction of the T_3 trimer is 345 times slower than the first phase of the reaction of the Cd(II)-T_6 hexamer [$k(T_1) = 19.0\ s^{-1}$] and 11.3 times slower than the second phase [$k(T_2) = 0.62\ s^{-1}$]. We attribute the slower reaction of the Cd(II) to the higher stability of the Cd−S bond. This result is an unambiguous and elegant evidence for the contribution of the metal ion−exogenous ligand interaction to the activation energy, proposed by Rahuel-Clermont et al. (*34*). The general principle postulates that hard acids prefer to coordinate to hard bases, while soft acids prefer to coordinate to soft bases. Our results show that the soft Lewis base (sulfur in KSCN) forms a strong bond with the soft Lewis acid Cd(II), thus lowering the energy of the ground state and increasing thereby the activation energy for the dissociation of the Cd(II)−insulin−thiocyanate complex. It has been proposed that the T_3 trimer in the T_3R_3 hexamer is less stable due to asymmetry in the T_3R_3 hexamer (*4*, *34*). Evidently, in the case of the Cd(II)-substituted hexamer, the increased affinity of sulfur to Cd(II) dominates the activation energy and more than compensates for the effects of asymmetry.

ACKNOWLEDGMENT

The author is grateful to Professor Michael F. Dunn (Department of Biochemistry, University of California, Riverside) for the use of the stopped-flow equipment in his laboratory and for time on the 500 MHz GN NMR spectrometer. The author thanks Dr. Niels C. Kaarsholm (Novo Nordisk, Copenhagen Denmark) for the generous gift of wild-type and mutant insulin used in this study and for providing the graphics-generated structure presented in Figure 5. The author thanks Dr. Ravi for recording the Mössbauer spectra and Dr. David G. Smith for stimulating discussions on structural details of the insulin hexamers.

REFERENCES

1. Baker, E. N., Blundell T. L., Cutfield J. F., Cutfield, S. M., Dodson, E. J., Dodson, G. G., Hodgkin, D. M. C., Hubbard, R. E., Isaacs, N. W., Reynolds C. D., Sakabe, K., Sakabe, N., and Vijayan, M. (1988) *Philos. Trans. R. Soc. London B 319*, 369−456.
2. Sudmeir, J. L., Bell, S. J., Storm, M. C., and Dunn, M. F. (1981) *Science 212*, 560−562.
3. Derewenda, U., Derewenda, Z., Dodson, E. J., Dodson, G. G., Reynolds, C. D., Sparks, C., and Swenson, D. (1989) *Nature 338*, 594−596.
4. Brzovic, P. S., Choi, W. E., Borchardt, D., Kaarsholm, N. C., and Dunn M. F. (1994) *Biochemistry 33*, 13057−13069.
5. Karatas, Y., Kruger, P., and Wollmer, A. (1991) *Biol. Chem. Hoppe-Seyler 372*, 1035−1038.
6. Smith, G. D., Swenson, D. C., Dodson, E. J., Dodson, G. G., and Reynolds, C. D. (1984) *Proc. Natl. Acad. Sci. U.S.A. 81*, 7093−7097.
7. Smith, G. D., and Ciszak E. (1994) *Biochemistry 33*, 1512−1517.
8. Bently, G. A., Brange, J., Derewenda, Z., Dodson, G. G., Markussen, J., Wilkinson, A. J., Wollmer, A., and Xiao, B. (1992) *J. Mol. Biol. 228*, 1163−1176.
9. Smith, G. D. and Dodson, G. G. (1992) *Proteins: Struct., Funct., Genet. 14*, 401−408.
10. Whittingham, J. L., Chaudhuri, S., Dodson, E. J., Moody, P. C. E., Dodson G. G. (1995) *Biochemistry 34*, 15553−15563.
11. Bentley, G. A., Dodson, E. J., Dodson, G. G., Hodgkin, D. C., Mercola, D. A., and Wollmer, A. (1975) Presented at the Spring Meeting of the British Diabetic Association, Sheffield, U.K.
12. Williamson, K. L., and Williams, R. J. P. (1979) *Biochemisrty 18*, 5966−5972.
13. Bradbury, J. H., and Ramesh, V., and Dodson, G. (1980) *J. Mol. Biol. 150*, 609−613.
14. Bradbury, J. H., and Ramesh, V. (1985) *Biochem J. 229*, 731−737.
15. Renscheidt, H., Strassburger, W., Glatter, U., Wollmer, A., Dodson, G. G., Mercola, D. A. (1984) *Eur. J. Biochem. 142*, 7−14.
16. Ramesh, V., and Bradbury, J. H, (1986) *Int. J. Pept. Protein Res. 28*, 146−153.
17. Wollmer, A., Rannefeld, B., Johansen, B. R., Hejnaes, K. R., Balschmidt, P. and Hansen, F. B. (1987) *Biol. Chem. Hoppe-Seyler 368*, 903−911.
18. Palmieri, R., Lee, R. W.-K., and Dunn, M. F. (1988) *Biochemistry 27*, 3387−3397.
19. Wollmer, A., Rannefeld, B., Stahl, J., and Melberg, S. G. (1989) *Biol. Chem. Hoppe-Seyler 370*, 1045−1053.
20. Kaarsholm, N. C., Ko, H.-C., and Dunn, M. F. (1989) *Biochemistry 28*, 4427−4435.
21. Roy, M., Brader, M. L., Lee, R. W.-K., Kaarsholm, N. C., Hansen, J. F., and Dunn, M. F. (1989) *J. Biol. Chem. 264*, 19081−19085.
22. Brader, M. L., and Dunn, M. F. (1990) *J. Am. Chem. Soc. 112*, 4585−4587.
23. Bloom C. R., Heymann, R., Kaarsholm, N. C., and Dunn, M. F. (1997) *Biochemistry 36*, 11638−11645.
24. Brader, M. L., Kaarsholm, N. C., and Dunn M. F. (1990) *J. Biol. Chem. 265*, 15666−15670.
25. Kruger, P., Gilge, G., Cabuk, Y., and Wollmer A. (1990) *Biol. Chem. Hoppe-Seyler 371*, 669−673.
26. Brader, M. L., Kaarsholm, N. C., Lee, R. W−K., and Dunn, M. F. (1991) *Biochemistry 30*, 6636−6645.
27. Brader, M. L., Borchardt, D., and Dunn, M. F. (1992) *Biochemistry 31*, 4691−4696.
28. Brader, M. L., Borchardt, D., and Dunn, M. F. (1992) *J. Am. Chem. Soc.114*, 4480−4486.
29. Choi, E. W., Brader, M. L., Aguilar, V., Kaarsholm, N. C., and Dunn, M. F. (1993) *Biochemistry 32*, 11638−11645.
30. Bloom, C. R., Choi, W. E., Brzovic, P. S., Ha, J. J., Huang, S.-T., Kaarsholm, N. C., Dunn, M. F. (1995) *J. Mol. Biol. 245*, 324−330.
31. Choi, E. W., Borchardt, D., Kaarsholm, N. C., Brzovic, P. S. and Dunn, M. F. (1996) *Proteins: Struct., Funct., Genet. 26*, 377−390.
32. Jacoby, E., Hua, Q. X., Stern, A. S., Frank, B. H., and Weiss, M. A. (1996) *J. Mol. Biol. 258*, 136−157.
33. Brader, M. L., Kaarsholm, N. C., Harnung, S. E., and Dunn, M. F. (1997) *J. Biol. Chem. 272*, 1088−1094.
34. Rahuel-Clermont, S., French, C. A., Kaarsholm, N. C., and Dunn, M. F. (1997) *Biochemistry 36*, 5837−5845.
35. Schlichtkrull, J. (1961) *Insulin Crystals: chemical and biological studies on insulin crystals and insulin zinc suspensions*, Novo, Copenhagen, Denmark.
36. Roy, M., Lee, R. W−K., Brange, J., and Dunn, M. F. (1990) *J. Biol. Chem. 265*, 5448−5452.
37. Kadima, W., Roy, M., Lee, R. W.-K., Kaarsholm, N. C., and Dunn, M. F. (1992) *J. Biol. Chem. 267*, 8963−8970.
38. Porter, R. R. (1953) *Biochem. J. 53*, 320−328.
39. Holyer, R. H., Hubbard, C. D., Kette, S. F. A., and Wilkins, R. G. (1966) *Inorg. Chem. 5*, 622−625.
40. Dunn, M. F., Bernhard, S. A., Anderson, D., Copeland, A., Morris, R. G., and Rogue, J.-P. (1979) *Biochemistry 18*, 2346−2354.
41. Dodson, E. J., Dodson, G. G., Hubbard, R. E., Moody, P. C. E., Turkengurg, J., Whittingham, J., Xiao, B., Brange, J., Kaarsholm, N., and Thøgersen, H. (1993) *Philos. Trans. R. Soc. London A 345*, 153−164.
42. Kadima, W. (1986*) NMR Studies of the Interaction of Cd(II) with Biological Ligands and Red Blood Cells*, Ph.D. Thesis, University of Alberta.
43. Theil, E. C., Eichhorn, G. L., and Marzilli, L. G., Eds. (1983) *Iron Binding proteins without cofactors or sulfur clusters*, Vol. 5 of Advances in Inorganic Biochemistry, Elsevier Science Publishing Company Inc., New York.
44. Cotton, F. A., and Wilkerson, G. (1988) *Advanced Inorganic Chemistry*, 5th ed., John Wiley & Sons, Inc., New York.
45. Finnegan, M. G., Kowal, A. T., Werth, M. T., Clark, P. A., Wilcox, D. E., and Johnson, M. K. (1991) *J. Am. Chem. Soc. 113*, 4030−4032.
46. Shriver, D.f., Atkins, P. W., and Langford, C. H. (1990) *Inorganic Chemistry*, pp 466−494, Oxford University press.
47. Bertini, I., Luchinat, C., Maret, W., and Zeppezauer, M., Eds. (1986) *Zinc Enzymes, Progress in Inorganic Biochemistry and Biophysics*, Vol. 1, pp 1−640, Birkhauser, Basel.

BI9903188